

**The Synthesis and Use of Iron Oxide Colloidal
Particles as the Support Material in HPLC**

by

Joseph Nitsche

A thesis submitted to the Faculty of the University of Delaware in partial fulfillment of the requirements for the degree of Honors Degree in Chemical and Biomolecular Engineering with Distinction

Spring 2015

© 2015 Nitsche
All Rights Reserved

**The Synthesis and Use of Iron Oxide Colloidal
Particles as the Support Material in HPLC**

by

Joseph Nitsche

Approved: _____
Mark R. Schure, Ph.D.
Professor in charge of thesis on behalf of the Advisory Committee

Approved: _____
Abraham M. Lenhoff, Ph.D.
Committee member from the Department of Chemical and Biomolecular
Engineering

Approved: _____
Susan Groh, Ph.D.
Committee member from the Board of Senior Thesis Readers

Approved: _____
Michael Arnold, Ph.D.
Director, University Honors Program

ACKNOWLEDGMENTS

I would like to thank the Undergraduate Research Department and the Honors Department for their guidance throughout the thesis process. I would also like to thank Mark Schure for his guidance throughout this research. He has been a great mentor to me over the last 2 years and has taught me to appreciate the wonders of chemistry and their applicability to solving a multitude of problems. I would also like to thank the Department of Chemical and Biomolecular Engineering for providing me with a world-class education that gave me the ability to conduct this research and write my thesis. Last, but not least, I would like to thank my entire family for their support of my education. I would especially like to thank my parents who have always supported my goals and sacrificed so much to help me achieve them and my sister, Hannah, who has taken this journey at the University of Delaware with me and been my best friend throughout the process.

TABLE OF CONTENTS

LIST OF TABLES	vi
LIST OF FIGURES	vii
ABSTRACT	x
1 Introduction	1
1.1 Motivation for Study	1
1.2 Utilization of Past Studies	2
1.2.1 Core-shell particle technology.....	2
1.3 Iron and Silica.....	3
2 Materials and Methods	5
2.1 Core Synthesis	5
2.1.1 Ellipsoid and Star Synthesis	6
2.1.2 Peanut Synthesis	10
2.2 Coating the Iron Cores.....	10
2.3 Multilayering: Creating the Pore Structure	11
2.4 Magnetization of Particles.....	13
3 Results and Discussion.....	16
3.1 Results of Ellipsoidal and Star Syntheses	16
3.2 Peanut Results	19
3.3 Impenetrable Silica Layer.....	20
3.4 Multilayering	24
3.5 Elutriation.....	28
3.6 Characterization of Colloidal Particles.....	33
3.6.1 FIB-SEM	33
3.6.2 Continuous Flow Steric Field-Flow Fractionator.....	36
3.7 Future Work.....	39

4	Conclusion.....	41
	REFERENCES.....	43

LIST OF TABLES

Table 1: Summary of conditions used for the synthesis of ellipsoidal particles.	7
Table 2: Summary of conditions used for the synthesis of 6 membered star particles.	9

LIST OF FIGURES

Figure 1: Phase diagram ³ for the conditions used to synthesize the ellipsoidal particles. E stands for ellipsoid, I for irregular particles, and N for no precipitation of particles.....	7
Figure 2: Phase diagram ³ for the conditions used to synthesize the six-membered star particles. The asterisks represent the star-shaped particles, N denotes no precipitation, the diamonds represent ellipsoidal-based particles, the squares represent hexagonal-shaped particles, and the circles represent spherical particles.....	9
Figure 3: Schmidlin NM-H2 500 hydrogen generator used to produce the hydrogen gas for the conversion of hematite to magnetite.....	14
Figure 4: Packed bed reactor used for the conversion of hematite to magnetite.....	14
Figure 5: SEM of the ellipsoidal particles synthesized with 0.05 M nitric acid and 0.02 M iron (III) nitrate aged for 72 hours shown at 10,000x magnification.....	16
Figure 6: Left: SEM of ellipsoidal particles synthesized using 0.05 M nitric acid and 0.02 M iron (III) nitrate aged for 72 hours. Right: SEM of ellipsoidal particles synthesized using 0.05 M nitric acid and 0.02 M iron (III) nitrate aged for 46 hours.....	17
Figure 7: SEMs of the six-membered star particles synthesized with 0.05 M perchloric acid and 0.026 M iron (III) chloride and aged 93 hours at 10,000x and 20,000x magnification.....	18
Figure 8: SEM of peanut particles at different magnifications (left: 5,000x and right: 20,000x).....	19
Figure 9: Peanut particles with the impenetrable silica coating at 10,000x magnification (left) and 20,000x magnification (right).....	21
Figure 10: SEMs of the scaled up coating of the peanut particles at 10,000x magnification (left) and 20,000x magnification (right).....	22
Figure 11: FIB-SEM of the coated peanut particles with an estimated shell thickness of 136 nm.....	23

Figure 12: SEM of the peanut particles after 3 steps of the multilayering process at 5,000x magnification (left) and 20,000x magnification (right).....	24
Figure 13: Number density plot from the Coulter measurement for the peanut particles before the multilayering process.	25
Figure 14: Number density plot for the pre-multilayer (red) and 6 th coat (green) Coulter counter results.....	26
Figure 15: Number density plot from the Coulter results for the 11 th and final coat of the multilayering process.	27
Figure 16: Number density plot from the Coulter results for the 11 th multilayer coat (red) and the sintered particles (green).....	28
Figure 17: Coulter counter results for drop 13 from the elutriation process.	29
Figure 18: Coulter counter results for drop 18 from the elutriation process.	30
Figure 19: Coulter counter results for drop 23 from the elutriation process.	31
Figure 20: Coulter counter results of drop 28 from the elutriation process.	32
Figure 21: Coulter counter results for the combined drops of 18-23 from the elutriation process.....	33
Figure 22: Left: FIB-SEM etching of an iron particle to determine the cross sectional dimensions of the particle. Right: FIB-SEM of an AMT core shell particles.	34
Figure 23: SEM of a core shell AMT particle that has undergone the multilayering process. Left is 20,000x magnification and right is 40,000x magnification.....	35
Figure 24: The fractionator supported on a frame with bearings allowing rotation under servo-motor control (on right). The initial design maintained that the sample collection was done in the blue-capped bottles shown above. That design was later modified to incorporate “in channel” sample collection as described below.	36
Figure 25: Schematic diagram of the CFStFFF system taken from reference 10.	37

Figure 26: The original apparatus including sample beaker (SB), magnetic stirrer (MS), pumps (P1-P3), carrier reservoir (CR), collection tubes (C1-8) first overflow (C9) and second overflow (C10). Arrows denote the flow direction. Taken from reference 10..... 38

ABSTRACT

High Performance Liquid Chromatography (HPLC) is a very important separation technique. This study attempted to create nonspherical iron oxide-based colloidal particles to be used as the cores in core-shell particles used as the support material for the stationary phase used in HPLC. The cores were coated with an impenetrable layer of silica to protect the cores from breaking down and to keep solutes away from iron. A porous layer was then added to the cores using a silica sol that were held together by a polymer. All of the colloids synthesized in this study were characterized using SEM and FIB-SEM. This study also included the creation of a Continuous Flow Steric Field-Flow Fractionator to be used to separate colloidal particles based on size, density, and shape.

Chapter 1

Introduction

1.1 Motivation for Study

HPLC or High Performance Liquid Chromatography is a very important and widely used separation technique in analytical chemistry. HPLC uses a stationary phase chemically bound to a support particle that is packed into a column and a mobile phase containing a given mixture of solvents that flows under pressure through the column. Each constituent of the mixture interacts differently with the stationary phase which causes each material to have a different velocity, leading to the separation. This study focuses on the stationary phase support material used in HPLC or more specifically the use of colloidal particles of different shapes for the stationary phase support. It was hypothesized that the use of particles with shapes other than spheres could be implemented into a column and provide unique packing properties. For the purpose of this study the performance of the particles synthesized for use in HPLC will not be discussed but will solely be the motivation and the driving force behind the research reported herein.

In order to prepare particles to be loaded into a chromatography column a certain set of properties had to be met. The goal was to create impenetrable cores of varying shapes and then coat the cores with a thin layer of silica. The thin layer of silica acts to protect the core from the materials in the mobile phase and the solute(s) to be separated from the core material. Once the cores were coated, a porous layer was added. This was done by adding a silica sol to the particles and the sol adhered to the

surface of the particles by various deposition methods. This was done in steps until the desired shell thickness was achieved. The pore structure of the particles was a very important part in the synthesis as the pore structure is what allows for the different materials in the mobile phase to interact with the stationary phase under optimal mass transport which is supported by using particles of the core-shell design. More specifically, the use of nonspherical particles of uniform shape may help mass transport in the fluid phase be rapid and more efficient than spheres in terms of availability of packed mass, and may offer better pressure relationships than spheres in reducing column backpressure.

1.2 Utilization of Past Studies

All of the syntheses and coating procedures used in this study were previously developed by other research teams. The originality of this research comes in combining multiple past studies to create unique core-shell particles with a porous outer layer. The use of the nonspherical particles of specific and regular shape in HPLC is also a unique idea that has not previously been studied. By combining the many syntheses and coating procedures a new and potentially improved way of constructing the stationary phase support in HPLC was created. It must be noted, however, that the chemical engineering process of producing many of these materials was never presented in the synthesis literature and many of those aspects are mentioned in this thesis.

1.2.1 Core-shell particle technology

One of the most recent realizations in analytical liquid chromatography is that core-shell based support materials have better mass transport properties than fully

porous particles^{1,2}. This is due to the reduction in diffusion length which occurs when a nonporous core is used as a support for a porous shell. The chemical stationary phase is then applied to the porous shell. Typically a spherical core-shell particle has an overall average diameter of 2.7 μm and a porous layer thickness of $\approx 0.5 \mu\text{m}$.

In the research performed here, attention is given to the synthesis and manipulation of the non-porous core particle whose geometry will affect the overall particle shape. The size and shape of this core will determine many of the mass transport properties through shape and size manipulation.

1.3 Iron and Silica

All of the colloids synthesized in this study were made of iron oxide, specifically hematite. The conversion of hematite particles to magnetite, so as to render the particles susceptible to a magnet, will be discussed below. The iron particles served as the cores in the core-shell particles. Iron was selected for multiple reasons. First, there has been a lot of research done on the synthesis of iron oxide colloids and publications exist for numerous different shapes of particles^{3,4,5,6}. The shapes of the cores was of particular interest in this study as there are well-documented procedures for the synthesis of iron oxide particles shaped like spheres, stars, rods, peanuts, cubes, etc. The iron oxide syntheses were also high yield syntheses which made them appealing. The last reason for the selection of iron was the potential to make the particles susceptible to magnetic fields. A number of applications exist for magnetic particles both in chromatography and in biological separations in bulk solution and many magnetic particle systems have been previously utilized^{7,8} for these applications. Silica was used to create the small impenetrable shell around the iron oxide core, used to chemically isolate the iron from the solute

molecules and to create the outer porous layer. Silica was chosen as it is generally chemically inert over a wide pH range which is important so different mobile phases do not break down the stationary phase nor support materials in the HPLC column.

Chapter 2

Materials and Methods

2.1 Core Synthesis

There were two main syntheses used in this research^{3,4}. Both syntheses involved the forced hydrolysis of iron (III) salts. Despite extensive research into these syntheses, little is known about the mechanism of the iron oxide precipitation process. Because of this, the directions for the creation of the particles were based on past successful syntheses. The shape of the final product depends significantly on the conditions of the synthesis. These conditions include: concentration of iron ions, pH, temperature, time of aging, and the type of anion present³. All of these conditions weigh heavily on the results of the synthesis and even the smallest change in any of them can result in colloidal particles of completely different shapes, which again led to the decision to recreate past syntheses.

All of the syntheses used a different iron salt and different acids and bases for the creation of the colloids. The choice of the iron salt depended on the desired shape of the particles. The iron salts were mixed with the acid/base and aged at elevated temperatures for extended periods of time. In this time the hydrolysis and the iron oxide synthesis occurred. All chemicals used here were available from Sigma-Aldrich (St. Louis, Missouri) except for the high-purity tetraethyl orthosilicate (TEOS) which was obtained from Advanced Materials Technology in Wilmington, Delaware.

2.1.1 Ellipsoid and Star Synthesis

The synthesis used to create the ellipsoid and star colloids was developed by Egon Matijevic *et al*³. The first step in the synthesis was to create high concentration stock solutions of iron salts (3 M) to prevent hydrolysis from occurring at room temperature. A predetermined amount of the iron salt was mixed with acid before dilution to the final volume. This was again done to prevent hydrolysis at room temperature. After dilution, the solution was transferred to 250 mL bottles, stoppered, and put in a laboratory oven at 100 °C for varying amounts of time. After removal from the oven, the particles were cooled to room temperature and washed 3 times with water and 3 times with ethanol by filtration using Millipore 0.45 µm filters. The particles were then dried at 50 °C for one hour before being put in bottles for storage.

The ellipsoidal particles used iron (III) nitrate as the iron salt and nitric acid. The phase diagram created by Matijevic *et al* is shown in Figure 1 and was used to determine the conditions used for the synthesis.

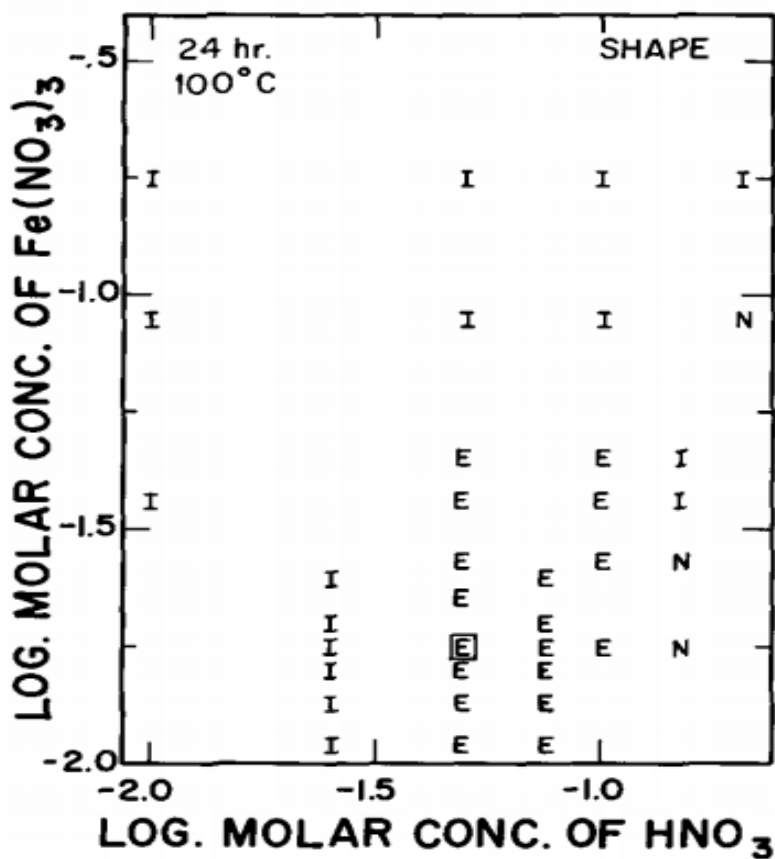


Figure 1: Phase diagram³ for the conditions used to synthesize the ellipsoidal particles. E stands for ellipsoid, I for irregular particles, and N for no precipitation of particles.

The phase diagram allowed for the desirable conditions for this study to be chosen. Table 1 shows all of the syntheses performed.

Table 1: Summary of conditions used for the synthesis of ellipsoidal particles.

Concentration Of HNO_3 (M)	Concentration of $\text{Fe}(\text{NO}_3)_3$ (M)	Oven Temperature °C	Oven Time (hours)
0.05	0.01	100	42
0.05	0.02	100	42

0.05	0.03	100	42
0.05	0.04	100	42
0.05	0.02	100	72
0.05	0.03	100	72
0.05	0.015	100	72
0.05	0.025	100	72
0.05	0.04	100	96
0.05	0.01	100	96
0.05	0.035	100	96
0.05	0.015	100	96

The six-membered star syntheses were performed in the same manner except the salt solution used was iron (III) perchlorate and the acid used was perchloric acid. The phase diagram for the stars was also generated by Matijevic *et al.* and is shown in Figure 2.

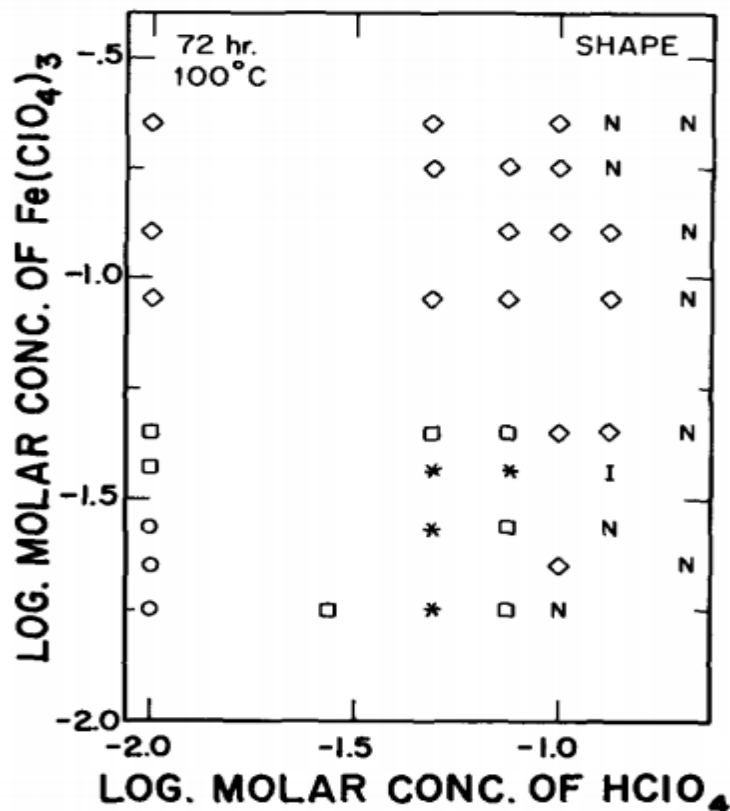


Figure 2: Phase diagram³ for the conditions used to synthesize the six-membered star particles. The asterisks represent the star-shaped particles, N denotes no precipitation, the diamonds represent ellipsoidal-based particles, the squares represent hexagonal-shaped particles, and the circles represent spherical particles.

The phase diagram was again used to determine the conditions for the syntheses in this study which are shown in Table 2.

Table 2: Summary of conditions used for the synthesis of 6-membered star particles.

Concentration of HClO ₄ (M)	Concentration of Fe(ClO ₄) ₃ (M)	Oven Temperature (°C)	Oven time (hours)
0.05	0.038	100	96
0.05	0.032	100	96

0.05	0.026	100	96
0.05	0.034	100	96

2.1.2 Peanut Synthesis

The peanut synthesis was very similar to the ellipsoidal and star syntheses except base was added to the solution instead of acid and was based on the work done by Yong Wang *et al*⁴. The iron salt used was iron (III) chloride and the base was sodium hydroxide. A typical synthesis started by creating 100 mL of 2 M iron (III) chloride. It was essential to stir the solution until the iron salt completely dissolved in solution. Failure to stir rigorously resulted in particles of undesirable shapes. 90 mL of sodium hydroxide was added to the solution drop-wise over 5 minutes while the solution was being stirred by a magnetic stir bar. Next 10 mL of 0.6 M sodium sulfate was added and the solution was stirred for an additional 10 minutes. The solution was then transferred to Pyrex bottles, stoppered, and put in an oven at 100 °C for 8 days. After 8 days the solutions were cooled to room temperature, cleaned 3 times with water, cleaned 3 times with ethanol, and dried at 50 °C for 1 hour. Scalability tests were performed to see if the synthesis could be scaled to 5-10 times the amount. This was done by simply increasing the amount of ingredients in equal molar ratios.

2.2 Coating the Iron Cores

The procedure for coating the iron cores with a small inert layer of silica was also based on work done by Yong Wang *et al*⁴. For a typical coating, 0.6 grams of dry iron particles were dispersed by ultrasonication in 100 mL of ethanol and 5 mL of deionized water. After the particles were suspended in the solution, 15 mL of NH₃·H₂O (28% in water) was added. The solution was transferred to a Pyrex bottle

and placed in an ultrasonication constant temperature bath at 50 °C. Next, 0.5 mL of TEOS was added and the solution was aged for 5 hours as the silica was produced by polymerization of the TEOS.

In order to be able to age the solution under ultrasonication and constant temperature an external bath system needed to be created. A 2 gallon bucket was used as the constant temperature bath. The bucket was filled with water and a copper heat-transfer coil was designed and placed in the bucket. Antifreeze was pumped through the coil using an external heating/cooling bath. A high frequency ultrasonication probe was submerged in the bath to create the desired conditions for the coating. It was important to keep the solutions under ultrasonication as TEOS has an affinity to react with itself and if the particles in the solution were not constantly mixed the TEOS would preferentially react and not achieve a uniform coating around the particles. Also without ultrasonication, the TEOS could react and stick to multiple particles at once and create a network of adjoined particles as opposed to separate and uniform particles.

2.3 Multilayering: Creating the Pore Structure

The idea behind the multilayering process is to add silica sol, which is comprised of small silica spherical particles, to the iron colloids. The silica sol adheres to the impenetrable shell and creates a layer. This is done over and over again until the sol creates a layer of desired thickness around the particles. This process creates a pore structure on the surface of the particles based on the imperfect packing ability of spheres and on layering with clusters (i.e. aggregates) of particles held together by a proprietary polymer system. The complete details of this process cannot be discussed

as much of it is a trade secret to the company Advanced Materials Technology, Inc., Wilmington, Delaware (AMT), with which this research is affiliated.

The first step in the process was to create and add 500 g of a polymer solution to a bottle filled with iron particles. The solution was then mixed for 20 minutes. The purpose of the polymer addition is to provide a means for the silica to adhere to and consequently coat the core which has a small layer of nonporous silica on the surface at this stage of particle preparation. The polymer first adheres to the surface of the particle and then to the silica sol when it is added. The solution was then centrifuged and mixed with a salt solution for 2 minutes, and centrifuged again. After decanting the salt solution, the particles are cleaned with DI water by centrifugation. The effluent was then decanted and the particles were mixed with the sol solution and mixed for 20 minutes. After mixing the particles were cleaned 3 more times with DI water. After the third cleaning the particles were ready for the next coat in which the procedure just described was repeated. The coatings were repeated until the desired pore structure thickness was achieved.

The thickness was monitored using a Beckman Coulter Multisizer. For this study an average of 12 coats were added to the particles. After the porous layer was determined to be the desired size, particles were cleaned with methanol 3 times and after the third cleaning they were filtered using a vacuum flask. The particles were then weighed and transferred to a vacuum oven at 110 °C and 0.7 bar. The particles were weighed every half hour until the mass stopped changing insuring the removal of the methanol from the particles.

The next step in the process was to burn off the polymer from the particles. This was done using a 24 hour program in a vented surface oven that ramped the

temperature from room temperature to 575 °C gradually. The final step in the process was to sinter the particles at 940 °C for 48 hours.

The particles were now elutriated using a proprietary elutriation system with 3 vessels. The flowrate was increased by 0.5-1 ml/min gradually. The bottoms of the elutriation apparatus were tested every hour to see what step the separation was at. Once the desired size range was achieved, the particles were dropped out of the collection vessel and then collected. Each volume of fluid released from the elutriation device was about 250 mL and each was caught in a separate container. All of the collections were tested for particle size using the Coulter counter and the decision was made as to what fractions to keep and which to discard.

The Coulter counter is a well-known device that can give very detailed and accurate particle diameters for spherical particles. Its use here is as a relative size detector. With rods and ellipsoidal-shaped particles, the readings are assumed to be that of a volume-averaged particle size. Hence the Coulter counter can detect increases in particle volume but does not give the aspect ratio or maximum size of a particle. Nonetheless, it is extremely useful as a control system when calibrated with known particle dimensions obtained by scanning electron microscopy (SEM) and image analysis software.

2.4 Magnetization of Particles

The conversion of hematite to magnetite is well studied and has been well documented by Itoh *et al* and Ozaki *et al*^{7,8}. The process used in this research, based on the known methods, was to pass hydrogen gas over a packed bed of hematite peanut particles at elevated temperatures. The hydrogen gas was produced in a Schmidlin NM-H2 500 hydrogen generator shown in Figure 3.

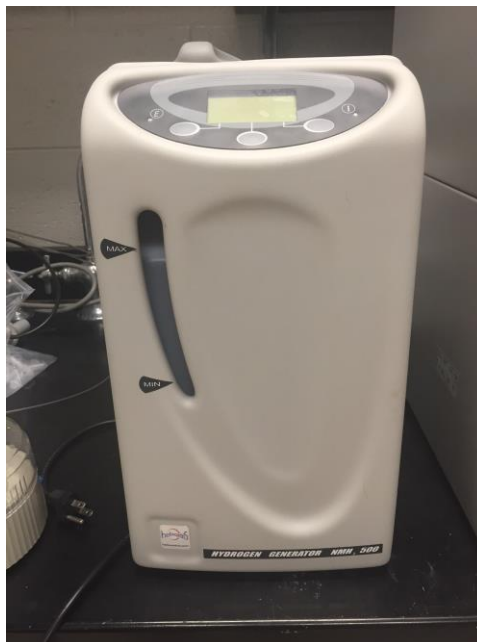


Figure 3: Schmidlin NM-H2 500 hydrogen generator used to produce the hydrogen gas for the conversion of hematite to magnetite.

The hydrogen gas was then fed to a stainless steel packed bed reactor that was fashioned specifically for this project. The packed bed reactor is shown in Figure 4. The reactor tube used in Figure 4 is a chromatographic column housing with 0.5 μm frits. All plumbing from the generator to the soap bubble flowmeter was comprised of 1/8 inch stainless steel tubing.

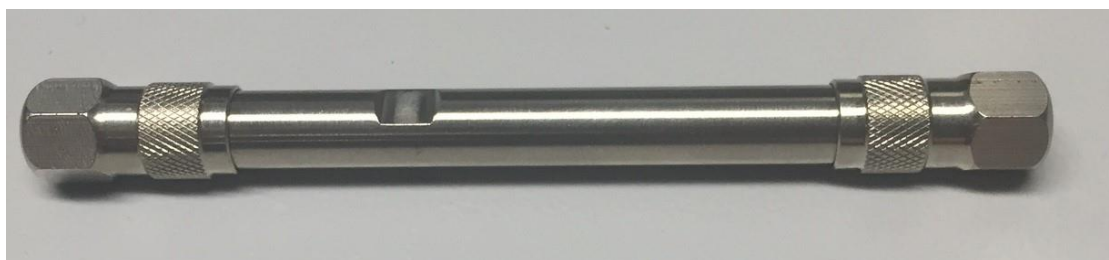


Figure 4: Packed bed reactor used for the conversion of hematite to magnetite.

The reactor was kept in an oven during the process to maintain a temperature of 250 °C. The hydrogen gas was continuously flowed into the reactor for 6 hours and the effluent gas was vented through a soap bubble flow meter into the hood. Upon cooling, the particles were found to be attracted to a magnet, hence verifying that the procedure worked. Note the literature reported higher temperatures for this process but it was found that the 250 °C condition worked fine and appeared to be complete.

Chapter 3

Results and Discussion

3.1 Results of Ellipsoidal and Star Syntheses

Once the syntheses were complete the main method of characterization was SEM. The first syntheses completed were the ellipsoidal particles and a typical SEM of these particles is shown below in Figure 5.

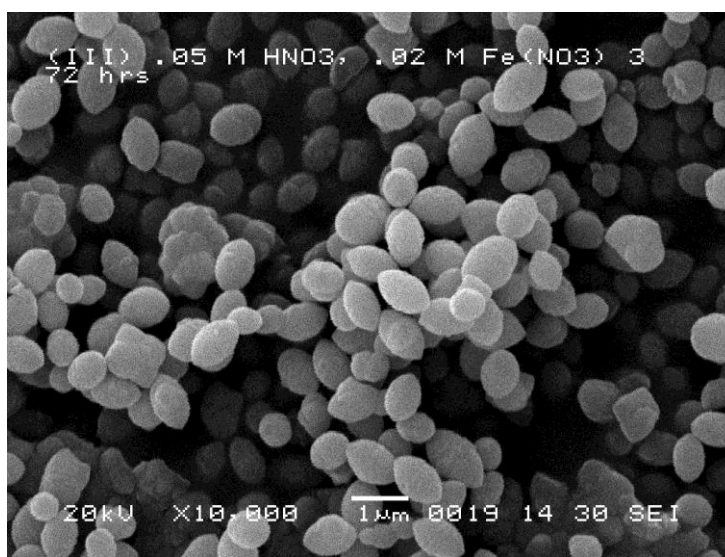


Figure 5: SEM of the ellipsoidal particles synthesized with 0.05 M nitric acid and 0.02 M iron (III) nitrate aged for 72 hours shown at 10,000x magnification.

The SEM micrograph shows that ellipsoids were almost entirely monodisperse with minor impurities. Tests were done to determine if the amount of time spent in the

oven affected the orientation and shape of the particles. If the same shape of particles could be achieved this would be desirable if this application ever reached a production type scale. Syntheses were completed with the same sets of conditions and the only change was the amount of time spent at the elevated temperatures. A typical SEM of these particles is shown in Figure 6.

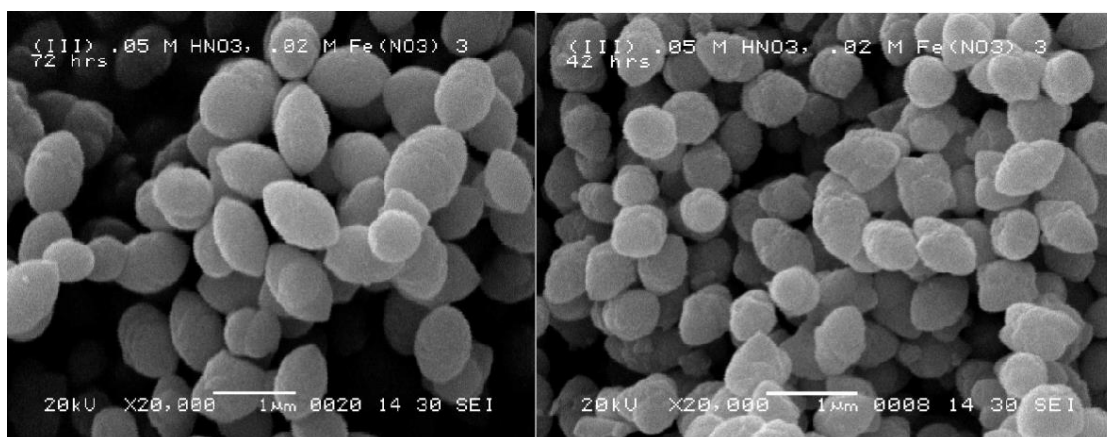


Figure 6: Left: SEM of ellipsoidal particles synthesized using 0.05 M nitric acid and 0.02 M iron (III) nitrate aged for 72 hours. Right: SEM of ellipsoidal particles synthesized using 0.05 M nitric acid and 0.02 M iron (III) nitrate aged for 42 hours.

Figure 6 shows that the particles on the left are much smoother and rid of impurities. The particles on the left were aged in the oven for 72 hours as opposed to the particles on the right that were aged for 42 hours at elevated temperatures. This proves that the amount of time spent in the oven is crucial to the formation mechanism of the colloids. Particles that were left in the oven for more than 72 hours did not appear to be any different than those left in for 72 hours. This set 72 hours as the minimum and optimal time for incubation.

SEMs were also taken of the star-shaped particles for characterization. A typical SEM of the star particles is shown below in Figure 7 at 2 different magnifications.

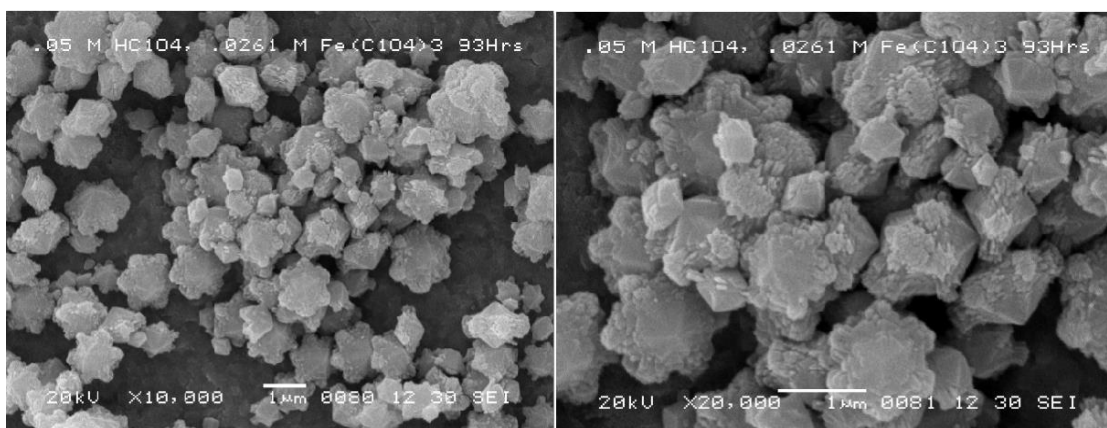


Figure 7: SEMs of the six-membered star particles synthesized with 0.05 M perchloric acid and 0.026 M iron (III) chloride and aged 93 hours at 10,000x and 20,000x magnification.

As can be seen from the images of the star-shaped particles, there were a lot of shapes other than stars and the surface of the particles were not smooth. These conditions were not conducive for adhering the nonporous silica shell to the outside of the particles. Also the impurities in the materials can be detrimental to the packing procedure for a chromatography column. When the particles are not uniform, the packing properties of the particles are affected and there is a chance that the particles do not pack efficiently which can affect the efficiency of the chromatography column.

For the star syntheses there were fewer sets of conditions tested. This arose from the preliminary SEMs, like those shown in Figure 7. The decision was made to neglect the star particles all together and focus on the ellipsoids. This is why no

temperature test was completed on the star-shaped particles. After further study a problem with the ellipsoidal particles arose as well. The yield, using a 250 ml bottle, was only about 0.25 grams on average. In order to pack a chromatography column about 3 grams of material is needed and multiple columns needed to be packed for testing. This realization led to the decision to search for new iron oxide syntheses that have higher yields and still produce nonspherical particles. This directed the research to the peanut syntheses.

3.2 Peanut Results

The main method of characterization of the iron (III) oxide cores shaped like peanuts was again SEM. The first SEMs taken were of the peanut particles after small bottle syntheses as described exactly by Wang *et al.* A SEM of the resultant particles is shown in Figure 8.



Figure 8: SEM of peanut particles at different magnifications (left: 5,000x and right: 20,000x)

As can be seen in Figure 8 the particles are very smooth and monodisperse. The yield of these syntheses was much greater than the yield of the ellipsoidal and star syntheses. A small bottle synthesis yielded anywhere from 3 to 5 grams of particles. Despite this high yield it was necessary to scale up to at least 1 liter batches so enough samples could be produced to perform tests on the particles. The scaling up process proved to be successful and the particles were just as monodisperse as the peanut syntheses before scale-up.

Now that the peanut synthesis was understood and provided monodisperse particles, the decision was made to move forward with the peanut particles. This entailed coating the peanut cores with the impenetrable silica layer and then using the multilayering process to create the pore structure and finished particles needed for chromatography column evaluation.

3.3 Impenetrable Silica Layer

The method for the creation of the impenetrable silica layer was first performed exactly as described by Wang *et al.* After the layer was applied, SEMs were taken and are shown in Figure 9.

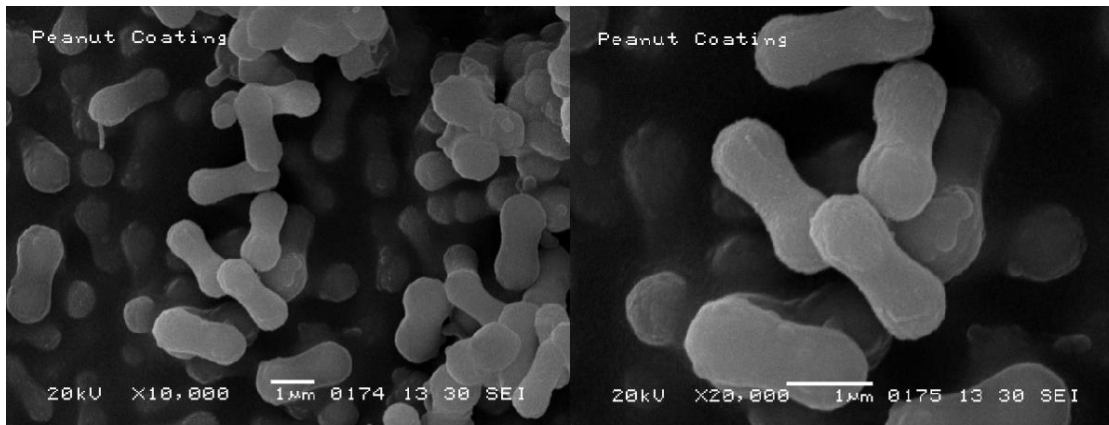


Figure 9: Peanut particles with the impenetrable silica coating at 10,000x magnification (left) and 20,000x magnification (right).

As Figure 9 shows, the particles appear to have small lumps on the surface that were not present before the coating. These abnormalities show that the coating was taking place; the silica was adhering to the iron. After the coating step the particles still appear to be monodisperse. The synthesis that was used was only based on the small bottle syntheses, thus the need for scale up was again present. The scale up required the creation of the external heat exchanger that was described in the methods and materials section. SEMs were taken after the scale up coating to insure that the process still worked. The SEMs of the scaled up coating are shown in Figure 10.

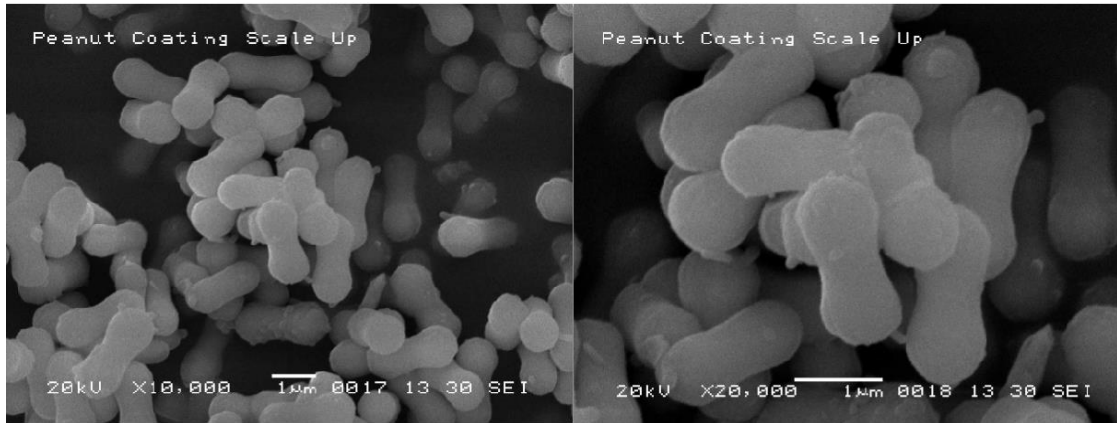


Figure 10: SEMs of the scaled up coating of the peanut particles at 10,000x magnification (left) and 20,000x magnification (right)

As Figure 10 shows, the particles have the same abnormalities on the surface as the particles in Figure 9. This supports the fact that the coating process still worked and the impenetrable layer was created around the iron core particles. In order to further show that the coatings were successful, Focused Ion Beam SEM (FIB-SEM) was performed. The images of the cross sections are in Figure 11.

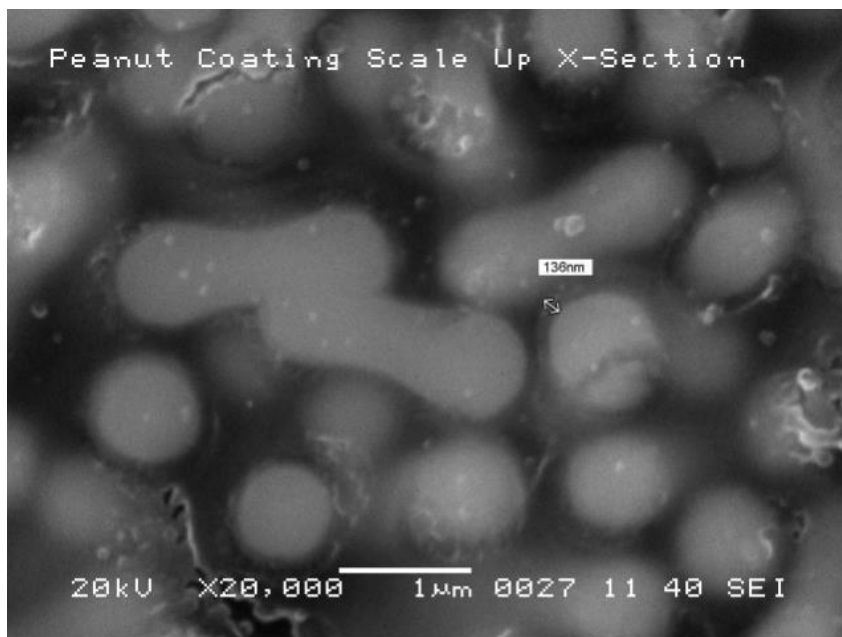


Figure 11: FIB-SEM of the coated peanut particles with an estimated shell thickness of 136 nm.

The FIB allows a particle to be “shaved” by the ion beam inside the vacuum system of the SEM. The particle’s cross-section is revealed in a much more controlled process than using a more traditional sample preparation process such as cutting an encapsulated sample with a diamond knife. The University of Delaware owns a FIB-SEM scope (a Zeiss Auriga 60 CrossBeam instrument) which is housed in the W. M. Keck electron microscope facility within the department of Materials Science and Engineering.

The particle that shows the 136 nm coating provides the best image of the coated layer where the faint ring around the outside of the peanut core is the silica shell. Now that it was possible to produce large quantities of coated peanut cores the multilayering step could be started.

3.4 Multilayering

The addition of the outer porous layer was the most crucial part to the particles' performance when packed into a chromatography column. SEMs were taken after 3 steps of the multilayering process to insure that the layers were adhering to the surface of the cores. Figure 12 shows the peanut particles after the 3 steps.

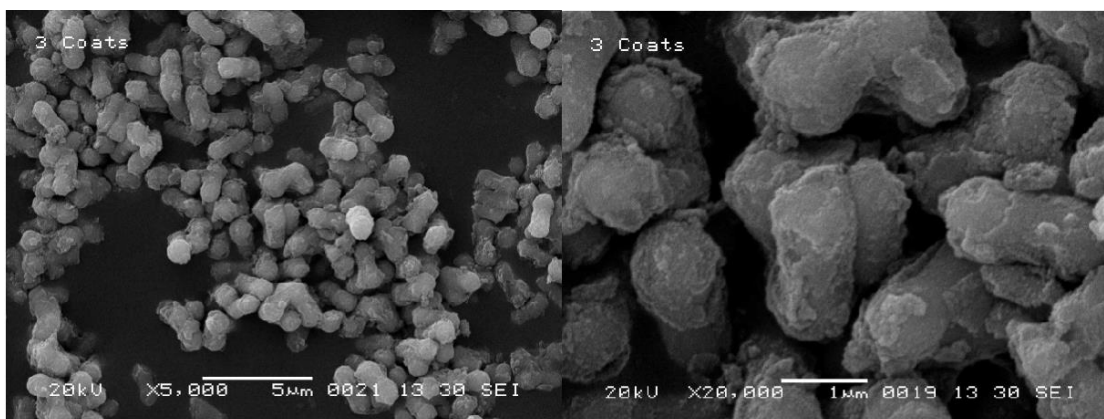


Figure 12: SEM of the peanut particles after 3 steps of the multilayering process at 5,000x magnification (left) and 20,000x magnification (right).

The particles in Figure 12 still take on the shape of the iron cores but there is a clear layer of silica forming on the surface of the particles. The multilayering process proved successful as the two main objectives were met. First, the particles did not adhere together when the silica sol was added. Instead the sol stuck to each particle individually and the unfavorable agglomeration of particles was avoided. Second, the peanut shape of the iron oxide core is still visible in the coated particles. The main goal of this research was to create nonspherical particles with superficially porous layers and therefore this synthesis appears to be successful. After showing that the process was working, more coats were added until the layer was grown to a

satisfactory size. The Coulter counter was used to keep track of the change in size of the particles.

As discussed previously in this thesis, the Coulter counter is calibrated to determine the diameter of a spherical particle. Therefore it is important to note that the readings from the Coulter counter for nonspherical particles are not exact measurements but rather a means to compare samples from different steps in the layering process. Coulter measurements were taken before the multilayering process began and after every step in the process. Figure 13 shows the results of the Coulter measurement taken before the first coat was applied.

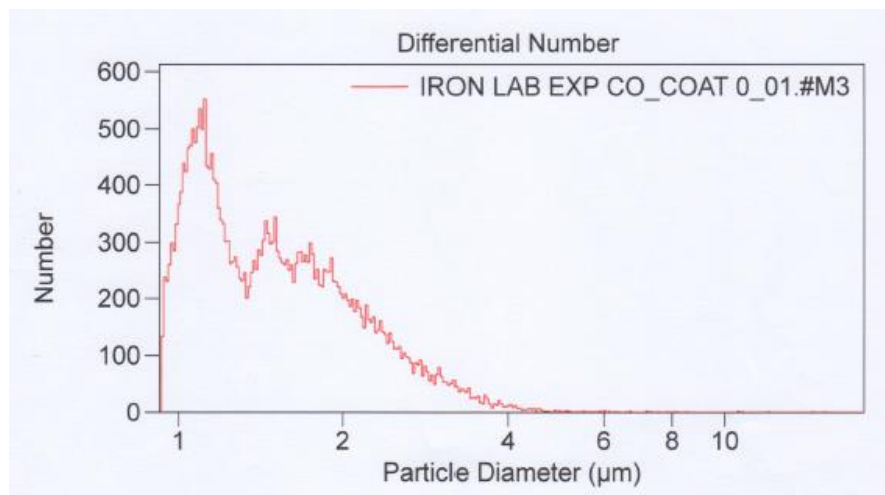


Figure 13: Number density plot from the Coulter measurement for the peanut particles before the multilayering process.

Figure 13 is a number density plot that shows the number of particles vs. the particle diameter. In this case, however, the particle diameter was treated as some characteristic length. It is believed that the two main peaks in the plot represent the

two orientations in which the peanut could pass through the orifice in the Coulter counter. The instrument could either be measuring the length of the particle with the first orientation or the width with the other main orientation, but “rotational averaging” makes these measurements difficult to interpret as definitive. In order to insure that the porous layer was growing with each step in the multilayering process, results from the Coulter counter were overlaid to show growth. Figure 14 shows the results from the 6th multilayer step and the pre-multilayer result.

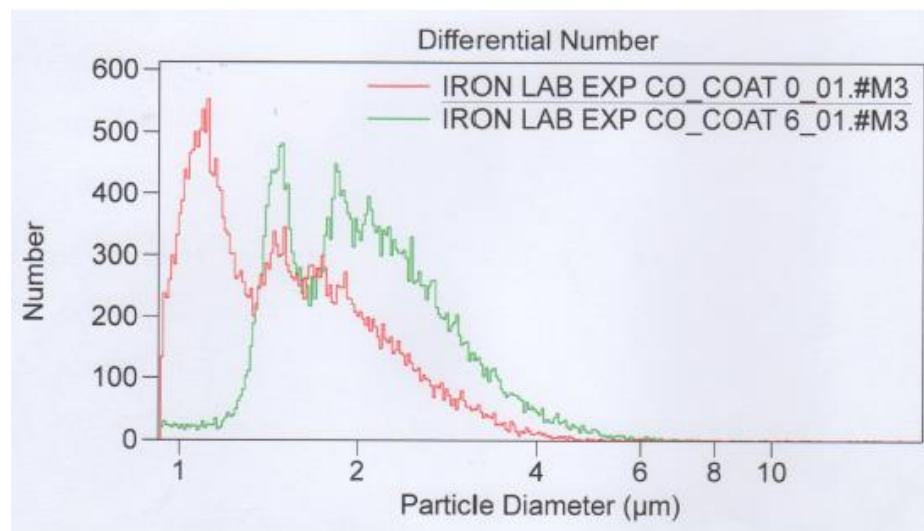


Figure 14: Number density plot for the pre-multilayer (red) and 6th coat (green) Coulter counter results.

Figure 14 shows that there was indeed growth after the first 6 steps in the multilayering process. Each characteristic peak grew by $\approx 0.5 \mu\text{m}$. The goal for the thickness of the porous layer was $\approx 1.0 \mu\text{m}$ and this was achieved after the 11th coat was applied. Figure 15 shows the Coulter results for the 11th coat.

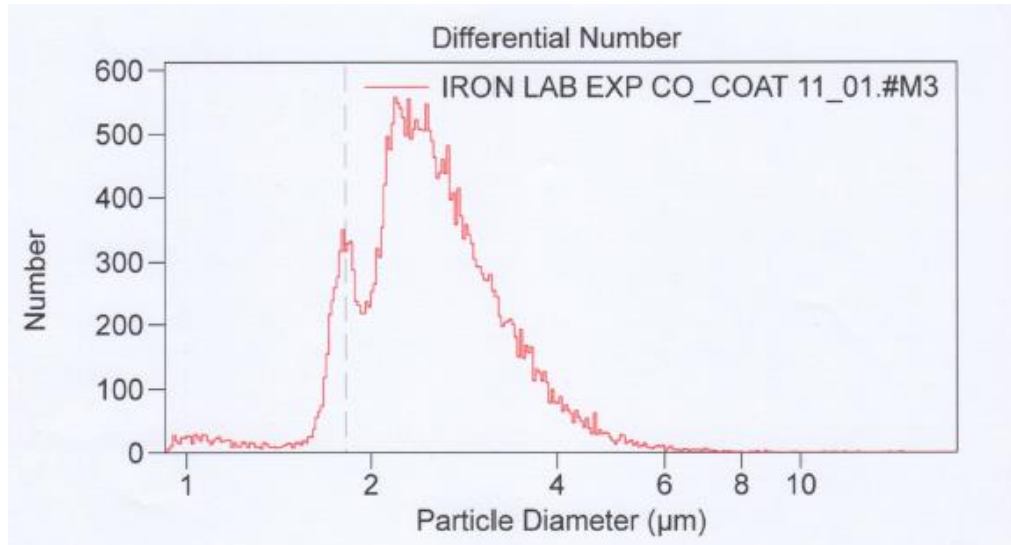


Figure 15: Number density plot from the Coulter results for the 11th and final coat of the multilayering process.

Figure 15 shows significant growth in the number of particles in the second characteristic peak. It is believed that this could have been caused by aggregation of individual particles. This unfavorable behavior will be eliminated in the elutriation process discussed below. After the 11th coat the first characteristic peak had grown by about 1 µm and thus the multilayering procedure was stopped.

After the multilayering process was complete, the particles were sintered to insure the porous layers had completely adhered to each other and to the iron core. Figure 16 shows the Coulter results for the sintered particles.

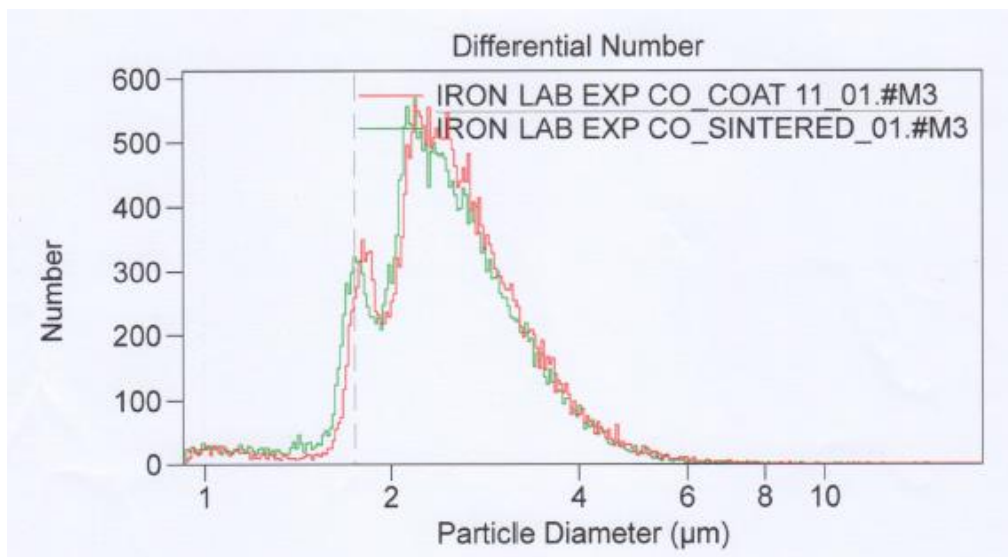


Figure 16: Number density plot from the Coulter results for the 11th multilayer coat (red) and the sintered particles (green)

Figure 16 shows that the characteristic peaks decreased slightly in size. This was expected because when the porous layer was exposed to such high temperatures the sol particles adhere together and form a more organized and tight porous network around the core.

3.5 Elutriation

The goal of the elutriation process was to remove the impurities from the particles and refine the width of the peak on the Coulter number density plots. This is important to the particle performance in HPLC as the particles may need to all be as close to the same size as possible for maximum performance. There were 38 drops made in the elutriation process and only 6 of them were used, drops 18-23. Figure 17 shows the Coulter results of drop 13.

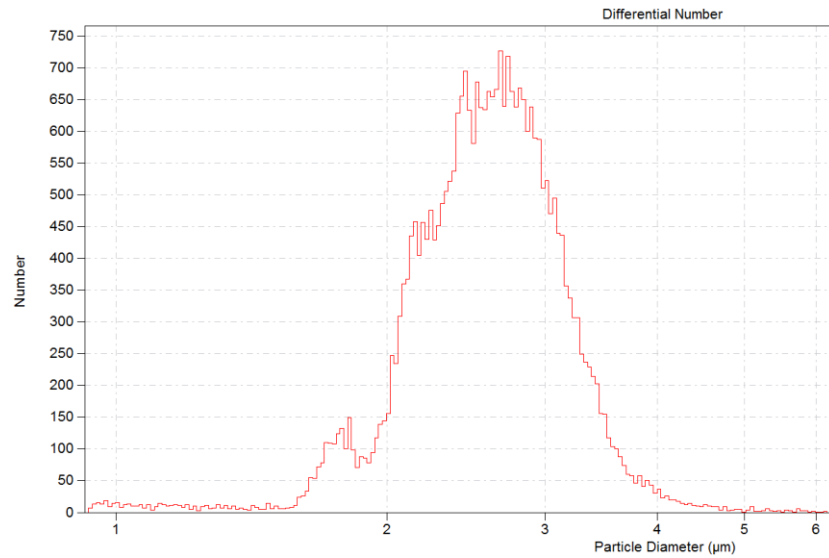


Figure 17: Coulter counter results for drop 13 from the elutriation process.

Figure 17 shows that there is one main large peak at about 2.75 µm. The target for the Coulter counter results was to have a narrow tall peak right above 2 µm. Figure 18 below shows the Coulter counter results for drop 18, which was the first usable drop from the elutriation process.

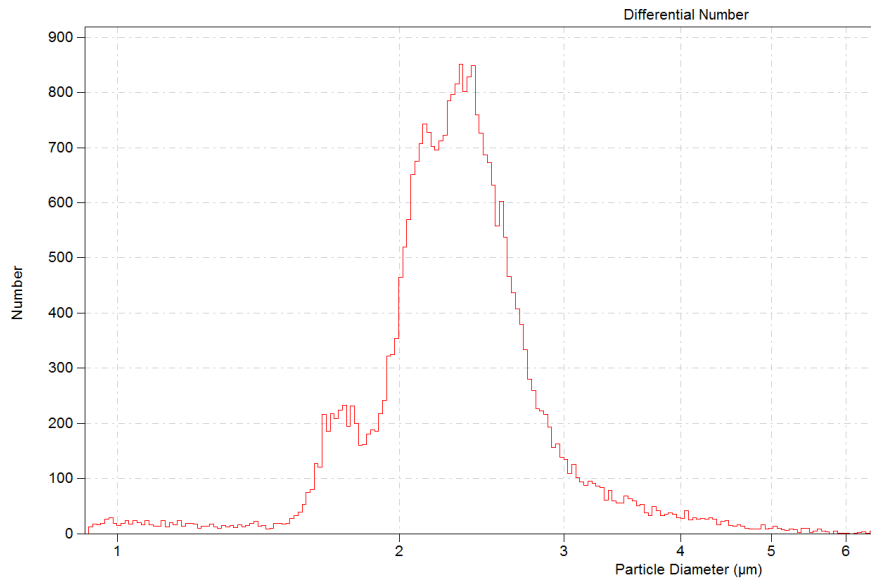


Figure 18: Coulter counter results for drop 18 from the elutriation process.

Comparing Figure 18 to Figure 17 the main peak greatly decreased in width and shifted towards the 2 μm point on the plot. This was the desired effect of the elutriation process. Drops 19-23 displayed similar behavior in their Coulter results. Figure 19 shows the Coulter counter results for drop 23, the last usable drop.

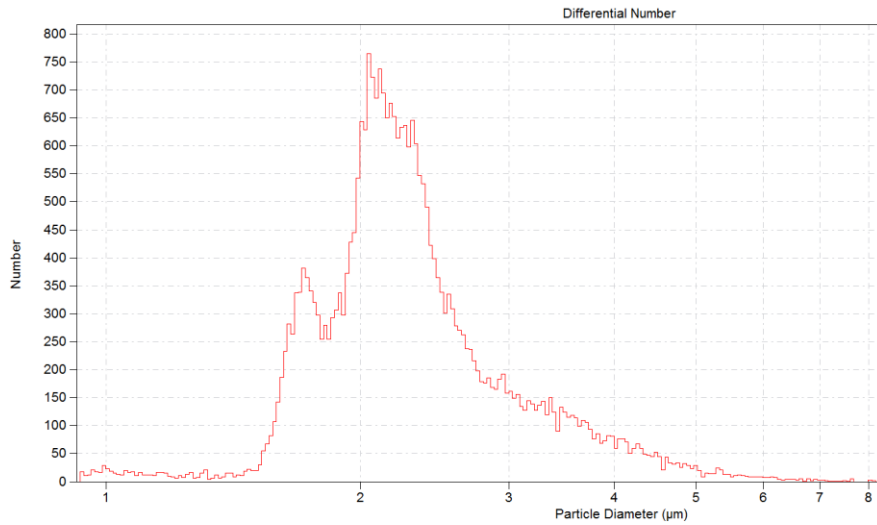


Figure 19: Coulter counter results for drop 23 from the elutriation process.

Figure 19 shows that the main peak has decreased in width even more and is still right around the 2 µm size. The difference between the results of drop 23 and 18 is the growing of the smaller peak on the left. This marked the end of the validity of the drops as this peak represents the possibility of particles that were not coated with every multilayer step. In order to visualize this even more the Coulter counter results from drop 28 are shown in Figure 20.

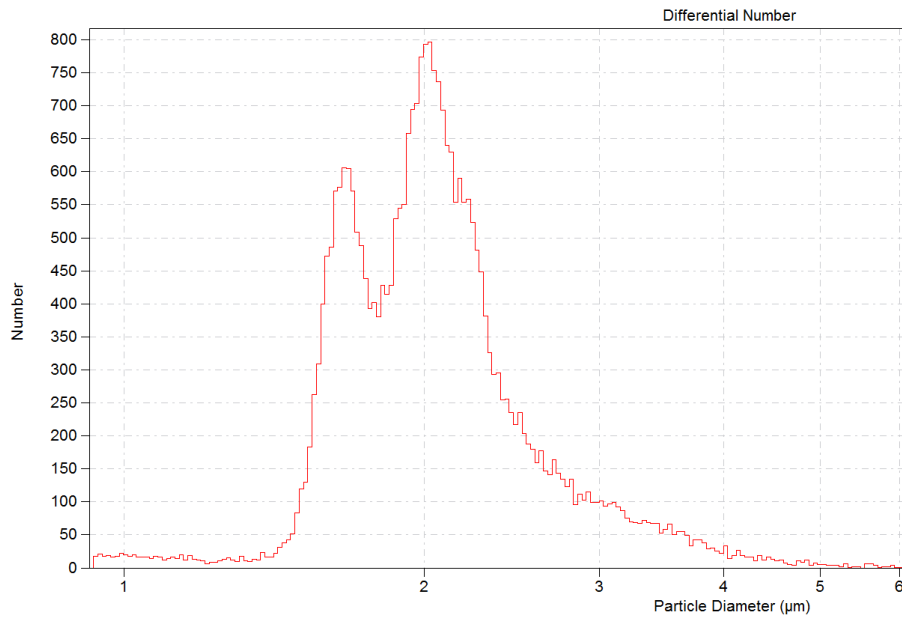


Figure 20: Coulter counter results of drop 28 from the elutriation process.

Drop 28 displays an even greater peak on the left and further confirmed the discontinuation of the drops at drop 23. All of the usable drops were combined and carried on to be used in the packing of a HPLC column. The Coulter counter results for the combined drops are shown in Figure 21.

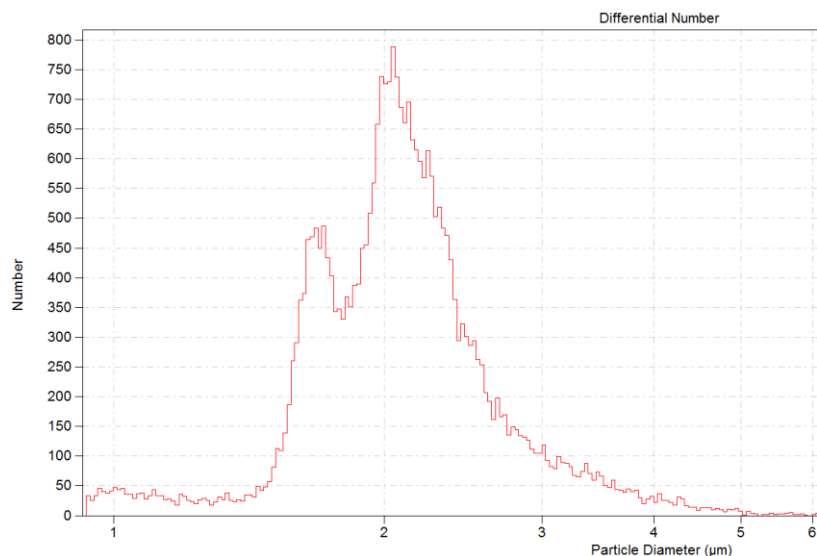


Figure 21: Coulter counter results for the combined drops of 18-23 from the elutriation process.

3.6 Characterization of Colloidal Particles

This research provided a unique opportunity to characterize all different shapes of colloidal particles. Many colloids were synthesized throughout this work other than the peanut particles that had interesting properties. One area of interest was in the pore structure of core shell particles with superficially porous layers. The goal was to investigate and characterize the pore structures using SEM and FIB-SEM. Another area of interest was to build and use a continuous flow steric field-flow fractionator to separate particles based on their size, shape and density.

3.6.1 FIB-SEM

FIB-SEM and SEM have been used throughout this work to characterize particles. FIB-SEM was used to take cross-sectional images to learn more about the core shell pore structure system.

As seen below in Figure 22 (left), the iron particle has a thin silica coating and ImageJ image analysis software (S3) was used to determine that this particle had a silica coating thickness of $\approx 50\text{-}70$ nm. This would have been extremely difficult to determine by sectioning of the particle population followed by SEM. FIB-SEM takes a few minutes to achieve pictures like this with subsequent image processing and little sample preparation. This method is also very applicable to spherical core-shell particles, as shown in Figure 22 (right).

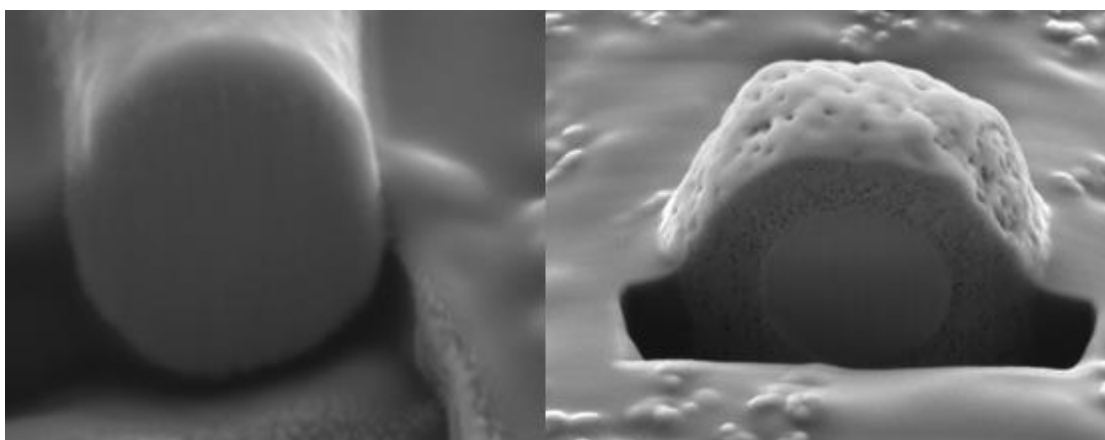


Figure 22: Left: FIB-SEM etching of an iron particle to determine the cross sectional dimensions of the particle. Right: FIB-SEM of an AMT core shell particles.

The main goal of the FIB-SEM work was to determine the pore structure configuration and see how the pores are connected and networked. This was attempted using overlapping FIB-SEM images, i.e. continuously slicing and imaging the particle over a period of time until the particle is completely etched away. After the images were taken, ImageJ was used to stack the images and make a video clip of the pore

structure being blasted away. This was not able to be completed with enough clarity and resolution to be reported in this thesis. However, this work is being continued with new procedures and new methods and guided by computer simulation of the imaging process.

SEM was also used to understand how the multilayering process works and how the sol particles adhere to the surface of a core and create a porous network. Figure 23 shows an image of an AMT core shell particle that clearly shows the small silica sol particles on the surface.

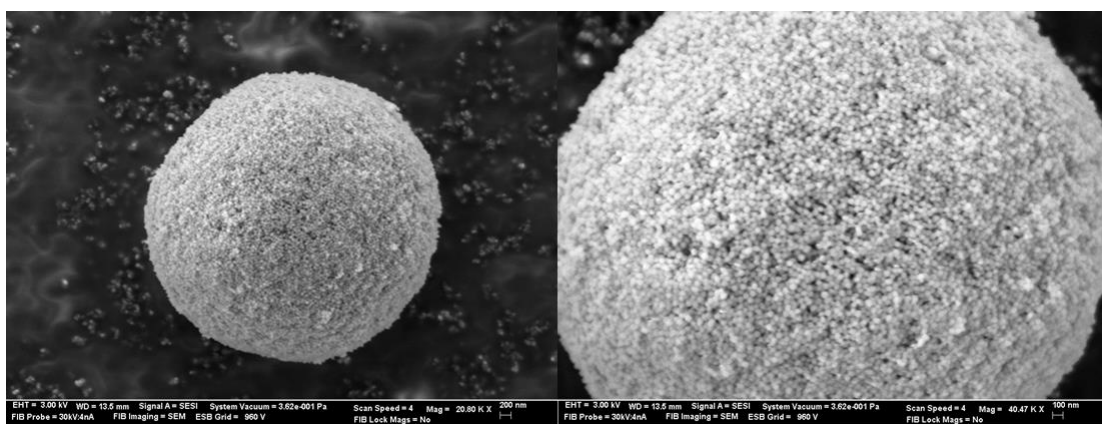


Figure 23: SEM of a core shell AMT particle that has undergone the multilayering process. Left is 20,000x magnification and right is 40,000x magnification.

Figure 23 shows that there are clearly small spherical sol particles on the surface. The sol particles have reacted with one another and adhered during a high-temperature sintering process. Their imperfect packing creates the pore structure in the core shell particle.

3.6.2 Continuous Flow Steric Field-Flow Fractionator

One of the aims here was to develop a more shape-sensitive method of separation on a semi-preparative scale. Towards this goal a continuous-flow steric field-flow fractionator was built, shown in Figure 24.



Figure 24: The fractionator supported on a frame with bearings allowing rotation under servo-motor control (on right). The initial design maintained that the sample collection was done in the blue-capped bottles shown above. That design was later modified to incorporate “in channel” sample collection as described below.

This device performs shape-based separations by sedimenting particles along a wall under a gravitational field shown below in Figure 25. Notice the channel is tilted. Channel flow also drives the particles into individual collection ports allowing for certain size, density and shaped particles to be collected. This device was invented by Myers and Giddings⁹ and utilized by Schure *et al*¹⁰ to separate complex particles of

environmental origin. No other usage of this technique has been found in the literature. The mechanism of separation is shown in Figure 25.

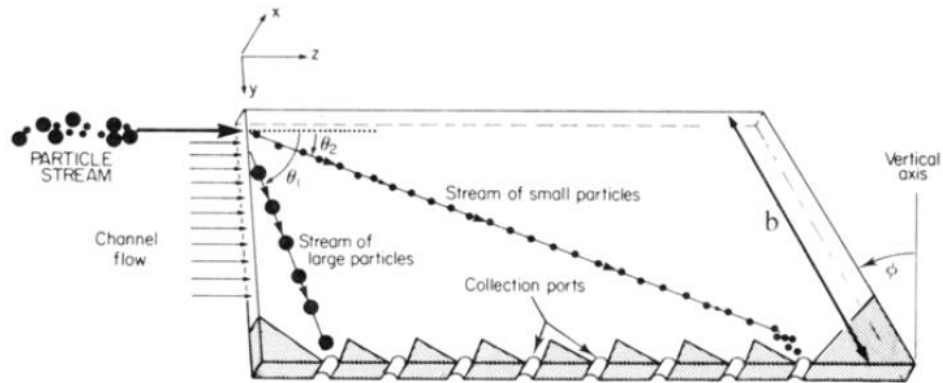


Figure 25: Schematic diagram of the CFISStFFF system taken from reference 10.

As can be seen in Figure 25, more dense particles will sediment faster as will larger particles. The equations have been worked out to guide experiment and they are quite simple^{9,10}. A desktop application is available that calculates which port the particles should collect at. The flow schematic used in this technique is shown in Figure 26.

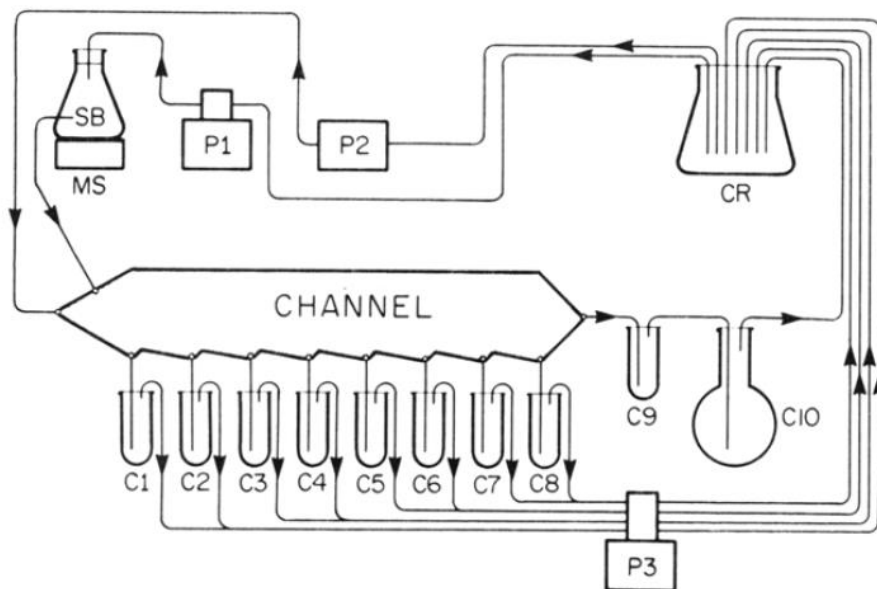


Figure 26: The original apparatus including sample beaker (SB), magnetic stirrer (MS), pumps (P1-P3), carrier reservoir (CR), collection tubes (C1-8) first overflow (C9) and second overflow (C10). Arrows denote the flow direction. Taken from reference 10.

The flow system in Figure 26 is from the original work^{9,10}. However, there were a number of modifications that were made as the instrument evolved. These modifications are listed here.

First, the collector point spacing is no longer uniform – i.e. equi-distant sample collection ports were utilized originally. This is not conducive to maximum resolution and the ports in this fractionator are spaced proportionally to $1/d$ where d is the particle size at constant density.

Next, to maintain the collection port flow at constant flow rate, restrictors were needed and the exit line from the collection bottles need to be “unpumped.” This fine adjustment and maintenance of flows is just too inflexible. The solution was to use nuts at the sample collection ports to close them and let samples accumulate within the

triangular (“sawtooth”) collection region formed between the walls and separated by the spacer system. Then when sample was accumulated and the run was complete, individual collection ports were emptied by opening the individual port and closing all others and applying flow. This approach is far simpler and much more efficient and will be automated with valves in the future.

Better shaped spacers are now being evaluated. Instead of using sawtooth-based shapes in the spacer, more capacity and less exposure to the flow field is had by using symmetrical and tapered collection ports with smooth curvature in the spacer and hence smooth curvature in the on-column collection regions.

The preliminary results of this experiment for fractionating silica and iron particles of specific shapes are still being clarified. However, it is felt that the future of this mode of characterization will simplify some of the characterization by particle shape in the future by utilizing the particle rolling mechanism on the wall. In addition, this device may aid magnetic particle characterization, whereby iron core particles have been rendered susceptible in a magnetic field (described in Section 2.4) and magnets can be added externally to the fractionator to guide the separation of magnetic particles from nonmagnetic particles based on size, shape and density.

3.7 Future Work

With all of the work and research done in this project there is still future work that can be done to carry on this work. The pore structure determination is one task that needs to be carried out. The goal of the FIB-SEM project was to get a video of the pore structure being etched away by the ion beam and run a computer simulation to model diffusion in the pores using the image stack as boundaries with quantitative

analysis of pore size and pore shape. This is a long sought-after goal for porous media and chromatography in particular.

Another area of research to be carried on is work with the fractionator. The fractionator was studied and constructed in this study but no particles have been run through the instrument to test its applicability to separation of particles based on size, density, and shape. Future experiments could mix some of the different shape colloids synthesized in this study and see if they are able to be separated based on size.

The last piece of this study to be finished in the future is the synthesis of more nonspherical shaped particles. The one synthesis that produced a high enough yield to be carried out through the coating and multilayering process was the peanut particles. Future studies could experiment with new syntheses to find particles with different shapes and higher yields that can also be coated and tested for use in HPLC specifically with a core-shell architecture that allows the geometry to be established by the shape and size of the core.

Chapter 4

Conclusion

HPLC is a very important separation technique used in analytical chemistry and attempts to improve the process are extremely important. This study used the work of past studies and known techniques to attempt to create innovative particles for use in the stationary phase support material of HPLC. The first step was to synthesize nonspherical particles made of iron (III) oxide, or hematite. Particles were synthesized in the shapes of ellipsoids, six-membered stars, and peanuts using previously developed syntheses. The next step was to coat the particles with a thin layer of silica to provide an impenetrable barrier to protect the integrity of the shape of the iron core and to isolate the solute(s) of interest from iron. The only particles that were carried on to this step in the process were the peanut shaped particles. After the impenetrable silica layer was applied, a porous structure was added to the outside of the core. The porous layer allows the particles to be bound with a stationary phase where the separation occurs due to different solute affinities for this phase. The porous layer was added using a multilayer process in which silica sol particles were added to the cores in a step-wise fashion to build up the size of the porous layer. The sol particles are held together by a polymer network. After the multilayer process the particles were elutriated to further refine the sizing of the particles.

Different methods were used to characterize the colloidal particles throughout this project. The main form of characterization was SEM and FIB-SEM. SEM was used in the synthesis phase to determine the shape and size of the particles. FIB-SEM

was used throughout the project to take images of the cross sections of particles and determine the dimensions of the silica layers on the outside of the iron cores. FIB-SEM was also used to attempt to produce a video of the etching of the pore structure from the surface of a core shell particle and to examine the network of pores.

A continuous flow steric field-flow fractionator was also created during this project. The goal of this instrument was to be able to separate colloidal particles based on size, density, and shape using the flow properties of the particles. This is a new application for this instrument as there very few references to the utilization of this type of separation in any other work.

This research developed a new way to think about creating the stationary phase support in a chromatography column. Nonspherical particles are not typically used in this application and the benefits from the packing properties of shapes other than spheres could greatly improve performance. The potential of using all different shapes and chemical makeups of colloidal particles for use in HPLC is endless. This study has only begun to scratch the surface of the opportunities in this area.

REFERENCES

1. Kirkland, J.J. Superficially Porous Supports for Liquid Chromatography, U.S. Patent 3505785, 1970.
2. R. Hayes, A. Ahmed, T. Edge, H. Zhang. (2014). Core-shell particles: Preparation, fundamentals and applications in high performance liquid chromatography. *Journal of Chromatography A*, 1357, 36–52
3. Matijevic, E., & Scheiner, P. (1978). Preparation of Uniform Particles by Hydrolysis of (Fe)-Chloride, -Nitrate, and -Perchlorate Solutions. *Journal of Colloid and Interface Science*, 63, 509-524.
4. Wang, Y., Su, X., Ding, P., Lu, S., & Yu, H. (2013). Shape-Controlled Synthesis of Hollow Silica Colloids. *Langmuir*, 29(37), 11575-11581.
5. Sugimoto, T., Khan, M. M., Muramatsu, A., & Itoh, H. (1992). Formation mechanism of monodisperse peanut-type α -Fe₂O₃ particles from condensed ferric hydroxide gel. *Colloids and Surfaces A: Physicochemical and Engineering Aspects*, 79, 233-247.
6. Sugimoto, T., Khan, M. M., & Muramatsu, A. (1993). Preparation of monodisperse peanut-type α -Fe₂O₃ particles from condensed ferric hydroxide gel. *Colloids and Surfaces A: Physicochemical and Engineering Aspects*, 70(2), 167-169.
7. H. Itoh, T. Sugimoto. (2003). Systematic control of size, shape, structure, and magnetic properties of uniform magnetite and maghemite particles. *Journal of Colloid and Interface Science*, 265, 283-295.
8. M. Ozaki, E. Matijevic (1985). Preparation and magnetic properties of monodispersed spindle-type γ -Fe₂O₃ particles. *Journal of Colloid and Interface Science*, 107 (1985), 199-203.
9. M. N. Myers, J. C. Giddings, A. (1979). Continuous Steric FFF Device for the size separation of particles. *Powder Technology*, 23, 15-20.
10. M. R. Schure, M. N. Myers, K. D. Caldwell, C. Byron, K. P. Chan, J. C. Giddings. (1979). Separation of Coal Fly Ash Using Continuous Steric Field-Flow Fractionation. *Environ. Sci. Technol*, 19, 686-689.

11. ImageJ is a highly popular public domain, open source image analysis software system developed at the National Institute of Health. See <http://imagej.nih.gov/ij/>